

O₂ chemisorption on CoO(100): A resonant-photoemission study

Shin-Puu Jeng, Zhaoming Zhang, and Victor E. Henrich

Surface Science Laboratory, Department of Applied Physics, Yale University, New Haven, Connecticut 06520

(Received 6 September 1990; revised manuscript received 11 March 1991)

The changes in the electronic structure of reduced single-crystal CoO(100) surfaces upon exposure to O₂ have been studied by means of resonant photoemission with use of synchrotron radiation. O-vacancy point defects on CoO(100) interact strongly with O₂ at room temperature. Ultraviolet photoemission difference spectra of the valence-band region taken before and after 10³ L of O₂ exposure (1 L ≡ 10⁻⁶ Torr sec) exhibit predominantly a 3d⁶-like final-state resonant behavior, which results from changes in substrate electronic structure arising from the reestablishment of Co-O ionic bonding on the surface upon O₂ exposure. Although most of the O₂ is believed to chemisorb as O²⁻, other adsorbed oxygen species are also present.

I. INTRODUCTION

Molecular chemisorption on 3d transition-metal oxide surfaces has been the subject of numerous studies, primarily owing to the technological importance of transition-metal oxides as heterogeneous catalysts, catalyst supports, and gas sensors.^{1,2} The adsorption of oxygen on the surfaces of oxides is particularly important since adsorbed oxygen species play a crucial role in the chemisorption of other molecules.² For example, molecular H₂O reacts with NiO surfaces only in the presence of chemisorbed oxygen.³ Also important for the interaction of molecules with oxide surfaces are the presence of surface defects and the valence state of the metal cations.^{1,2,4} In general, the surfaces of nearly perfect maximal valency oxides are inert to most molecules at room temperature, while chemisorption is strong on defective surfaces. O-vacancy point defects are the predominant surface defects observed on these ionic oxides.¹ When a surface O²⁻ ion is removed from the lattice, roughly two electrons must be trapped at the defect site in order to maintain local charge neutrality; these excess electrons partially populate the normally empty 3d orbitals on the cations adjacent to the defects, resulting in an increase in the degree of covalent bonding on the surface.

One of the most perplexing chemisorption systems that has been encountered in single-crystal studies on transition-metal oxides is the interaction of O₂ with defective surfaces of the rocksalt transition-metal monoxides MnO,⁵ CoO,⁶ and NiO.³ Creation of O-vacancy point defects on the (100) surfaces of those oxides appears in ultraviolet photoemission spectra (UPS) as emission in the bulk band gap just above the valence band maximum, either as a broadening of the upper edge of the valence band or as distinct shoulders on the band edge. When photoemission difference spectra are taken for O₂ exposures ≤ 10³ Langmuir (i.e., when the ultraviolet photoemission spectrum for an atomically clean surface is subtracted from spectra for the same surface after molecular adsorption.^{1,3,5-9}), the dominant feature is a large negative peak (or peaks) near the valence band maximum cor-

responding to the (generally complete) depopulation of the defect surface states. The remainder of each difference spectrum consists of relatively weak, structureless positive emission across the region of the valence band further than about 1 eV below the valence band maximum (see Fig. 3 below for CoO). It has been difficult to correlate this emission with either the molecular orbitals of adsorbed species or changes in the density-of-states of the surface. This is in contrast to results for the early 3d transition-metal oxides TiO₂, SrTiO₃, and Ti₂O₃, where distinct features appear in the difference spectra in the region of the O 2p valence band.¹

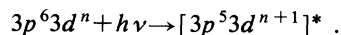
Both the bulk electronic properties of CoO and the interaction of O₂, CO, and H₂O with CoO(100) have been previously investigated.^{6,10,11} We have recently used resonant photoemission to study the creation of O-vacancy defects on CoO(100).¹⁰ The CoO(100) surface is a good prototype for the rocksalt transition-metal monoxides in that O-vacancy point defects can be created on the surface while still maintaining the overall geometric order of the surface, as determined by low-energy-electron diffraction (LEED). The data indicate that the creation of O-vacancy defects reduces the number of ionic Co—O bonds on the surface, in conjunction with the increase in the degree of covalent bonding at the defect site. In the present paper we report the use of resonant photoemission to monitor the adsorption of O₂ onto defective CoO(100) surfaces. We show that the difference spectra correspond predominantly to changes in the substrate electronic structure that arise from the reestablishment of Co—O ionic bonding on the surface upon O₂ exposure.

II. RESONANT PHOTOEMISSION IN TRANSITION-METAL OXIDES

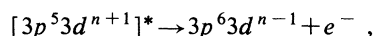
The direct (nonresonant) photoelectron emission of *d* electrons from the valence orbitals of transition-metal compounds, which occurs for all photon energies, can be expressed

$$3d^n + h\nu \rightarrow 3d^{n-1} + e^- .$$

However, when the photon energy is greater than the cation $3p \rightarrow 3d$ optical absorption threshold, which occurs at 62 eV for CoO,¹² an alternative excitation process becomes possible. The photon can excite a cation $3p$ electron into a normally empty $3d$ level



The resulting excited state decays via a super-Coster-Kronig process^{13,14}



resulting in the same as that of the direct emission process. Interference between the two processes results in a resonant behavior of the amplitude of the d -orbital emission as the photon energy is varied across the $3p \rightarrow 3d$ threshold.

The resonant photoemission process is ion selective, and in transition-metal oxides there are no optical absorption thresholds for the O²⁻ ion in the photon energy range used to excite the cation $3p \rightarrow 3d$ excitation. Thus any resonant effects are associated with the cations, or with the cation contribution to wave functions of hybridized bands. But the process has been found to be even more selective than that. For stoichiometric CoO, the ground-state wave function can be expressed in a configuration interaction picture as¹³

$$\Psi_g = a|3d^7\rangle + b|3d^8\bar{L}\rangle + c|3d^9\bar{L}^2\rangle ,$$

where \bar{L} denotes a $2p$ hole on an otherwise O²⁻ $2p^6$ oxygen ligand. The d^7 term represents the ionic component of the interatomic bonding, while the $d^8\bar{L}$ and $d^9\bar{L}^2$ terms correspond to the covalent part of the bond. The final state wave function, after one electron has been emitted, can be written as

$$\Psi_f = \alpha|3d^6\rangle + \beta|3d^7\bar{L}\rangle + \gamma|3d^8\bar{L}^2\rangle .$$

The $3d^6$ final state can be derived only from the $3d^7$ ionic ground state, without any charge transfer from ligand p to cation d orbitals. The $3d^7\bar{L}$ charge-transfer final state can be obtained either by direct $3d$ electron emission from the $3d^8\bar{L}$ ground state or by final-state charge-transfer screening of the $3d^6$ state.^{15,16} As has been demonstrated for Cu, Ni, and Fe compounds having n $3d$ electrons in the ground state,¹³ the $3d^{n-1}$ final state exhibits a strong Fano-type resonance in the cation $3d$ photoemission intensity near the $3p \rightarrow 3d$ threshold, with the intensity largest for photon energies slightly above threshold. On the other hand, the intensity variations of the $3d^n\bar{L}$ and $3d^{n+1}\bar{L}^2$ final-state emission are relatively weak and exhibit an antiresonance dip (rather than a peak) as the photon energy is increased across the threshold. For this reason it has been possible to monitor the changes in the degree of ionic bonding on CoO(100) surfaces as a function of O-vacancy defect creation.¹⁰

Resonant photoemission can also be used to study the electronic structure changes that take place upon adsorption. The emission due to the adsorbate-induced electronic structure changes in the $3d$ orbitals of CoO(100) will be enhanced across the resonance, while any unhybridized molecular orbital emission from the adsorbate

will not be enhanced. Clear differentiation between these two types of emission is certainly important for characterizing the chemisorption on oxide surfaces, but it has been difficult to achieve by using only a single-energy photon source such as He I or He II. In this paper we report the use of tunable synchrotron radiation to assist in differentiating substrate and adsorbate features in photoemission difference spectra.

III. EXPERIMENTAL PROCEDURE

A single crystal of CoO was oriented and cut into rods of 4×4 mm² cross section having the (100) face normal to the rod axis. The sides of the cleavage rod were coated with ~ 0.5 μm of Al in order to reduce charging during photoemission measurements. The nearly perfect CoO(100) surface was produced by cleaving the sample *in situ* in the spectrometer vacuum chamber at a base pressure below 2×10^{-10} Torr; surface defects were created by bombarding the surface with 500 eV Ar⁺ ions. All of the adsorption experiments were carried out at room temperature, and both the O₂ and CO used in this study were obtained from Matheson as research grade, and each had a purity of 99.99%. The resonant photoemission experiments were performed on beamline U14 at the National Synchrotron Light Source, Brookhaven National Laboratory. Photons were incident at an angle of 45° to the (100) surface normal, and angle-integrated photoemission spectra were measured with a Physical Electronics 15-255G double-pass cylindrical-mirror analyzer (CMA) whose axis was oriented 45° to the (100) surface. In spite of the insulating nature of bulk CoO, no charging was observed in measurements at room temperature on Al-coated samples. For each spectrum in which the photon energy was varied, the photocurrent of a Au grid flux monitor was used to correct for variations in light intensity from the monochromator. Because the photoemission spectra are shifted with respect to the Fermi energy by different amounts for different surface treatments such as Ar⁺-ion bombardment and O₂ exposure, all of the spectra (except Fig. 1) have been aligned with the spectral feature at 1.5 eV binding energy in Fig. 1.

IV. RESULTS

Figure 1 presents the valence band photoemission spectra of cleaved CoO(100) taken at photon energies of 60 eV (just below threshold) and 62 eV (just above threshold); both spectra are referenced to the Fermi energy. Although there is strong cation-anion hybridization throughout the valence band in CoO, features at binding energies of 5.0 and 7.6 eV are primarily due to O $2p$ emission. Other features, at binding energies of 1.5, 3.7, and 10.4 eV, are primarily $3d$ -derived features. The bottom spectrum is the difference between the spectra above and below resonance; it thus represents mainly the contribution of the $3d^6$ -final-state-derived features to the UPS. Because the Coulomb interaction between the $3d$ hole created in the photoemission process and the other cation $3d$ electrons is not strong enough in CoO to widely separate different electronic configurations,¹⁵ and since

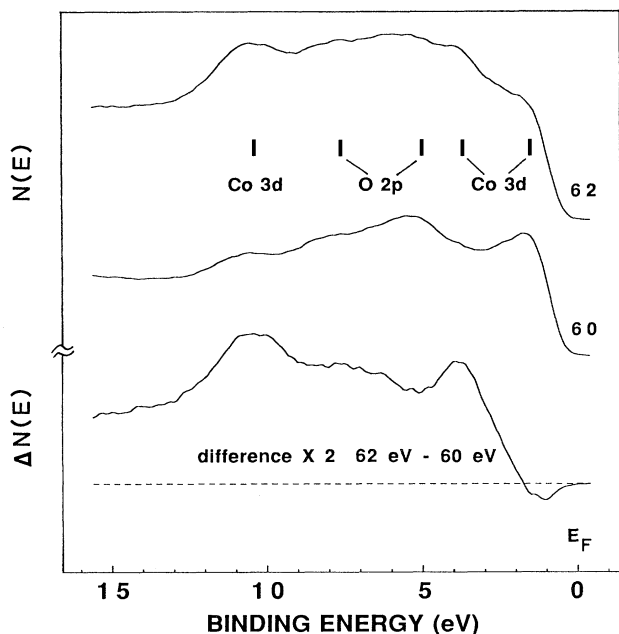


FIG. 1. Angle-integrated valence-band photoemission spectra of UHV-cleaved CoO(100) measured at photon energies of 60 and 62 eV, showing resonant enhancement of the 3d states. The (62 eV-60 eV) difference spectrum (bottom trace) reflects primarily the distribution of the 3d⁶ final state; the vertical scale for the difference spectrum has been expanded by a factor of 2. The features indicated on the 62-eV spectrum have binding energies of 1.5, 3.7, 5.0, 7.6, and 10.4 eV.

the screening dynamics of the 3d hole are more complex than those of a core hole in XPS,¹⁵ the energy distribution of the 3d⁶ final state is wide (~12 eV). Most of the unhybridized O 2p contribution as well as features involving ligand-to-metal charge transfer are removed from the difference spectrum since their intensities do not change much with photon energy. Note, for example, that the feature at 1.5 eV does not appear in the difference spectrum; there is even a slight decrease in its amplitude at 62 eV photon energy, consistent with its origin as a charge-transfer state.^{10,11} Based upon the difference spectrum shown in Fig. 1, the features at binding energies of 3.7 and 10.4 eV constitute the dominant contributions from the 3d⁶ final state.

Oxygen vacancies and other more complex surface defects are produced by Ar⁺-ion bombardment as a result of energy and momentum transfer to the surface; this results in the net removal of O ions from the surface.¹⁷ After bombardment to steady state by 500 eV Ar⁺ ions, the CoO(100) surface still displays a LEED pattern, although the beams are broader and the background intensity higher than for the cleaved surface.⁶ This indicates that the surface retains a high degree of its original geometrical order. It has been shown that slightly more than 4% of a monolayer of surface oxygen ions are removed from the CoO(100) surface during this process; thus, isolated O vacancies are expected to be the dom-

inant type of surface defect on this slightly reduced CoO(100) surface.^{6,10} The changes caused by Ar⁺-ion bombardment in the valence band photoemission spectrum of CoO(100) can be seen in Fig. 2, which is taken at 62 eV photon energy in order to maximize the sensitivity to the ionic contribution of the bonding. There is a decrease in the emission between 1 and 12 eV binding energy, accompanied by the appearance of a distinct feature at the upper edge of the valence band due to the creation of surface defects. The defect-related feature at the upper edge of the valence band does not exhibit any resonant behavior as a function of photon energy.¹⁰

The changes that occur in the valence band photoemission as the defective CoO(100) surface is exposed to O₂ at room temperature are shown in the upper three spectra in Fig. 3 for $h\nu=62$ eV. In agreement with the study of chemisorption on CoO(100) by Mackay and Henrich,⁶ oxygen interacts strongly with the defective surface, resulting in the disappearance of the surface defect feature in the photoemission spectrum after only ~10 L of oxygen exposure. The changes that result from somewhat higher oxygen exposure can be seen in the difference spectra at the bottom of Fig. 3, where the clean surface spectrum has been subtracted from the spectrum for 10³ LO₂ exposure. The solid curve is the difference spectrum for $h\nu=62$ eV, while the dashed curve was taken with $h\nu=60$ eV. Both spectra shows a large decrease in the emission of the surface defect feature, accompanied by an overall increase in emission between 1 and 12 eV binding energy. The largest positive feature in the difference spectra occurs at ~10.4 eV. Only a single chemisorbed oxygen phase is observed on CoO(100) between 0 and 1000 L of O₂ exposure, consistent with previously reported results.¹¹

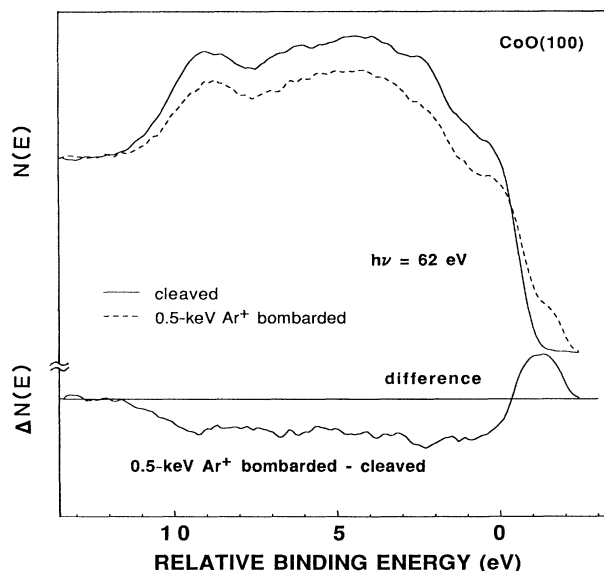


FIG. 2. Photoemission spectra ($h\nu=62$ eV) of cleaved CoO(100) before (solid curve) and after (dashed curve) bombardment with 500 eV Ar⁺ ions, and the difference spectrum between the two.

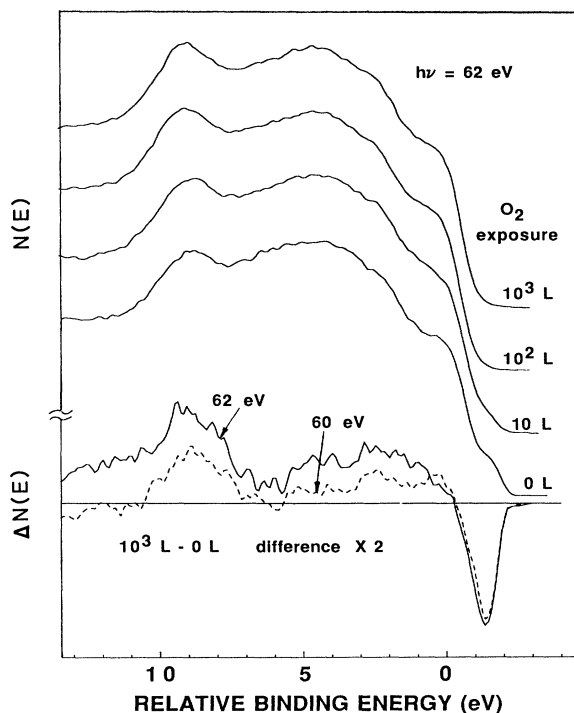


FIG. 3. Photoemission spectra ($h\nu=62$ eV) of 500 eV Ar^+ -ion-bombarded CoO(100) as a function of oxygen exposure at room temperature. The difference spectra (1000 L-0 L) for $h\nu=62$ eV (solid curve) and 60 eV (dashed curve) show the changes caused by the interaction of O_2 with defective CoO(100); the vertical scale for the difference spectra has been expanded by a factor of 2.

V. DISCUSSION

A. Defect creation on CoO(100)

As has been discussed previously, the creation of O-vacancy defects on CoO(100) results in a decrease in the degree of ionic bonding on the surface and the creation of covalent cation-cation bonding at defect sites.¹⁰ The positive peak in the difference spectrum in Fig. 2 corresponds to emission of electrons from the covalent bonds at defect sites; thus it does not resonate as a function of $h\nu$. The negative region corresponds to a decrease in all types of electron emission as O ions are removed from the surface, but since the spectra are taken at $h\nu=62$ eV, the largest contribution to the difference will be made by the $3d^6$ component of the final state, which is the only one that is derived solely from the ionic $3d^7$ initial state. The amplitude of the decrease in emission upon defect creation is significantly larger than 4%, which is roughly the fraction of O ions removed by ion bombardment. The reason for this is that the removal of one O ion not only eliminates its ionic bonds, but also changes the character of the bonding in the vicinity of the defect.

B. Effects of O₂ chemisorption

Since the defective CoO(100) surface is oxygen deficient, O_2 is expected to dissociate for low exposures, removing electrons from the defect sites to create negative adsorbed O species. The changes induced by such a charge transfer process associated with O_2 chemisorption at defect sites are, qualitatively, a reversal of the changes that occur for ion bombardment of the stoichiometric surface, as can be seen by comparing the difference spectra in Figs. 2 and 3. But the changes in the difference spectra in Fig. 3 as the photon energy is varied from below to above the resonance energy give a more detailed picture of the nature of the adsorption. The resonant enhancement of the difference spectra is evident (i.e., nearly a twofold increase in intensity for the 62-eV spectrum compared to the 60-eV spectrum), indicating that the difference spectra contain predominantly the changes in substrate electronic structure arising from the reestablishment of Co-O ionic bonding on the surface upon oxygen exposure,¹⁰ since the $3d^6$ final-state emission features are the ones that resonate most strongly as the photon energy is varied.

The changes in the UPS upon O_2 exposure can be seen in a somewhat different way in Fig. 4, which shows the differences taken between spectra that are above and below the resonance threshold for both ion-bombarded and subsequently O_2 -exposed CoO(100) surfaces, and for the cleaved CoO(100) surface. The shapes of all three difference spectra are the same, since, no matter how many different types of bonding are present on the surface, this type of difference spectrum isolates the ionic contribution. The overall intensity of the difference spectrum is reduced after ion bombardment of the cleaved surface, indicative of a reduction in the number of ionic

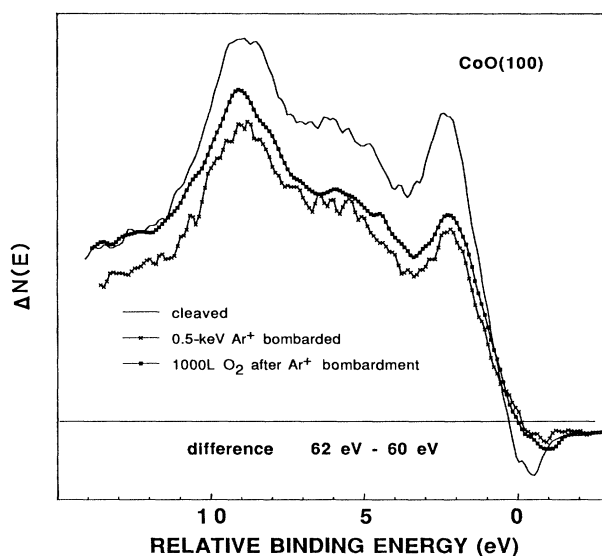


FIG. 4. Comparison between the (62 eV-60 eV) photoemission difference spectra for the (a) cleaved, (b) 500 eV Ar^+ -ion-bombarded, and (c) then 1000 L O_2 exposed surfaces.

Co—O bonds on the defective surface.¹⁰ After 1000 L of O₂ exposure, the intensity of the difference spectrum for defective CoO(100) increases, although it is never as large as that for the cleaved surface, even though the band gap emission associated with electrons localized at surface defect sites has been eliminated. Thus O₂ exposure has only partially restored the ionic Co—O bonding on the bombarded surface.

While the ultraviolet photoemission difference spectra presented here clearly show that many of the O₂ molecules interact dissociatively with defect sites, becoming O²⁻ species and therefore reestablishing some surface Co²⁺—O²⁻ ionic bonding, other types of chemisorbed oxygen species are present as well. This can be seen in UPS taken at lower photon energies where the cross-section for O 2*p* excitation is larger and where the structure in the valence band is better defined. Figure 5 compares the photoemission spectra from cleaved CoO(100) with that from the defective surface after exposure to O₂ for $h\nu=45$ eV. Virtually all oxygen on the cleaved CoO(100) surface consists of lattice oxygen having very nearly an O²⁻ configuration. The differences between the two spectra can thus arise from two sources. Either some of the adsorbed O species have a molecular orbital structure different than that of O²⁻, or the disorder that remains on the surface after ion bombardment causes significant changes in the occupied density of states. (Angle-dependent photoemission effects resulting solely from changes in surface geometry should not be very pronounced here since the spectra are semi-angle-integrated.) While it is not really possible to separate these effects, the fact that the differences in the two spectra in Fig. 5 occur primarily in the region of the valence band that is dominated by O 2*p* orbitals (compare with Fig. 1) suggests the presence of chemisorbed oxygen in states other than nor-

mal lattice O²⁻. The present data do not allow any more definitive determination of the additional species adsorbed except to note that it is probably not O⁻, since the partially filled oxygen 2*p* orbital in O⁻ would presumably give rise to some feature in the difference spectra only slightly below the Fermi energy, and no such feature is observed.

C. Comparison with other transition-metal oxides

The chemisorption of oxygen on the insulating transition-metal oxides TiO₂,^{8,9} and SrTiO₃,⁹ has been observed to occur in at least two phases: the first phase exhibits a large sticking coefficient for O₂ exposures between 0 and ~10² L, while a second phase, having a much smaller sticking coefficient, occurs for higher O₂ exposures. Similar two-phase oxygen chemisorption has also been reported to occur on some heavy 3*d* transition-metal oxides like NiO,³ CoO,⁶ Fe₂O₃,⁷ and MnO;⁵ however, the spectral distinction between various chemisorption phases on these oxides is less clear than that on TiO₂ and SrTiO₃. In the present study, only a single phase of chemisorbed oxygen is obtained for oxygen exposures between 0 and 1000 L. It is interesting to note that, in spite of the differences in the electronic structure among NiO, CoO, Fe₂O₃, and MnO, the chemisorption of oxygen on these oxides generally results in similar difference spectra, such as the one shown in Fig. 3 for low exposures, suggesting a similar type of oxygen interaction for all of these 3*d* transition-metal oxides.

In addition to the low-exposure regime addressed here, O₂ chemisorption on transition-metal oxides for higher oxygen exposures (e.g., ≥ 10⁶ L) should also be investigated in detail using resonant photoemission. Even for light 3*d*-transition-metal oxides, where the first chemisorbed phase is presumably understood, higher exposures yield ultraviolet photoemission difference spectra that have never been properly interpreted. A wide range of assignments of adsorbed species exists in the literature; charged species such as O₃⁻, O₂⁻, O₂²⁻, and O⁻, and neutral species like O₂, have all been considered previously for high-exposure O₂ chemisorption.^{5-9,18-22}

VI. SUMMARY

The interaction of O₂ with defective single-crystal CoO(100) surfaces has been studied using synchrotron radiation and resonance photoemission. The resonance effects that occur as the photon energy is varied through the cation 3*p*→3*d* optical excitation threshold permit separation of the changes in the electronic structure of the substrate as a result of interaction with the adsorbate from emission from the occupied molecular orbitals of the adsorbed species. The slightly defective (i.e., reduced) CoO(100) surface interacts strongly with O₂ at room temperature. Ultraviolet photoemission difference spectra of the valence band region taken before and after O₂ exposure exhibits a 3*d*⁶-like final-state resonant behavior, which results from the reestablishment of Co—O ionic bonding on the surface upon O₂ exposure. Although it is concluded that most of the chemisorbed oxygen on the

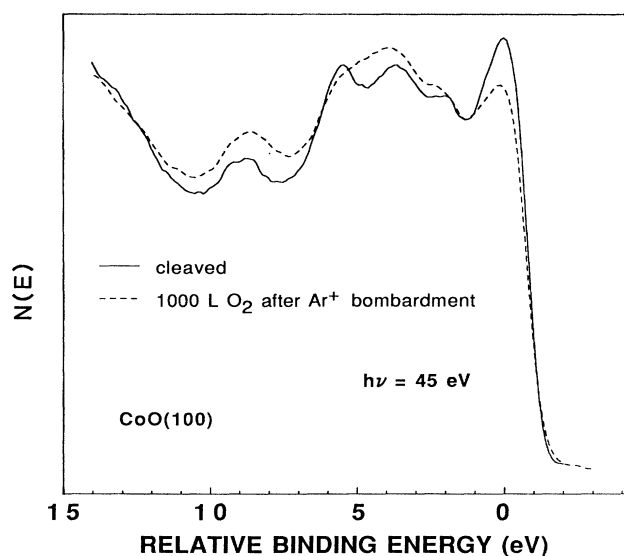


FIG. 5. Photoemission spectra ($h\nu=45$ eV) of cleaved CoO(100) (solid curve), and for 1000 L oxygen exposure of the bombarded surface (dashed curve).

defective CoO surface exists as O²⁻, the degree of ionic Co—O bonding on the surface only partially recovers compared to that of the cleaved surface. The reduced ionicity of the O₂-exposed defective surface is attributed to the presence of chemisorbed oxygen at defect sites in phases other than lattice O²⁻.

ACKNOWLEDGMENTS

The authors would like to thank the staff of the National Synchrotron Light Source for helpful technical as-

sistance and Professor Yasuo Sakisaka of Kyoto University for kindly supplying the CoO crystal. Useful discussion with Dr. J. S. Ledford and Dr. R. L. Kurtz are gratefully acknowledged. This work was partially supported by NSF Solid State Chemistry Grant No. DMR-87-11423, and by DOE Office of Basic Energy Sciences Grant DE-FG02-87ER13773. Research was carried out at the National Synchrotron Light Source (Upton, N.Y.), which is supported by the Department of Energy, Division of Materials Sciences and Division of Chemical Sciences Grant DE-AC02-76CH00016.

- ¹V. E. Henrich, Rep. Prog. Phys. **48**, 1481 (1985); V. E. Henrich, in *Proceedings of the NATO Advanced Study Institute on Defects in Solids: Modern Techniques*, edited by A. V. Chadwick and M. Terenzi (Plenum, New York, 1986), p. 311; V. E. Henrich, in *Surface and Near-Surface Chemistry of Oxide Materials*, edited by Dufour and Nowotny (Elsevier, Amsterdam, 1987), p. 23.
- ²H. H. Kung, *Transition Metal Oxides* (Elsevier, Oxford, 1989).
- ³J. M. McKay and V. E. Henrich, Phys. Rev. B **32**, 6764 (1985).
- ⁴T. Wolfram and S. Ellialtioglu, in *Theory of Chemisorption*, edited by J. R. Smith (Springer-Verlag, Berlin, 1980), p. 149.
- ⁵R. J. Lad and V. E. Henrich, J. Vac. Sci. Technol. A **6**, 781 (1988); R. J. Lad and V. E. Henrich (unpublished).
- ⁶J. L. Mackay and V. E. Henrich, Phys. Rev. B **39**, 6156 (1989).
- ⁷R. L. Kurtz and V. E. Henrich, J. Vac. Sci. Technol. A **2**, 842 (1984); R. L. Kurtz and V. E. Henrich, Phys. Rev. B **36**, 3413 (1987).
- ⁸W. J. Lo, Y. W. Chung, and G. A. Somorjai, Surf. Sci. **71**, 199 (1978).
- ⁹V. E. Henrich, G. Dresselhaus, and H. J. Zeiger, J. Vac. Sci. Technol. **15**, 534 (1978).
- ¹⁰S.-P. Jeng and V. E. Henrich, Solid State Commun. **75**, 1013 (1990).
- ¹¹Z. X. Shen, J. W. Allen, P. A. P. Lindberg, D. S. Dessau, B. O. Wells, W. Ellis, J. S. Kang, S. J. Oh, A. Borg, I. Lindau, and W. E. Spicer, Phys. Rev. B **42**, 1817 (1990); Z. X. Shen, C. K. Shih, O. Jepsen, W. E. Spicer, I. Lindau, and J. W. Allen, Phys. Rev. Lett. **64**, 2442 (1990).
- ¹²R. Bruhn, B. Sonntag, and H. W. Wolff, J. Phys. B **12**, 203 (1979).
- ¹³See, for example, A. Fujimori and F. Minami, Phys. Rev. B **30**, 957 (1984); S. J. Oh, J. W. Allen, I. Lindau, and J. C. Mikkelsen, *ibid.* **26**, 4845 (1982); L. C. Davis, *ibid.* **25**, 2912 (1982); G. van der Laan, Solid State Commun. **42**, 165 (1982); A. Fujimori, M. Saeki, N. Kimizuka, M. Taniguchi, and S. Suga, Phys. Rev. B **34**, 7138 (1986); A. Fujimori, N. Kimizuka, M. Taniguchi, and S. Suga, *ibid.* **36**, 6691 (1987); A. Kakizaki, K. Sugeno, T. Ishii, H. Sugawara, I. Nagakura, and S. Shin, *ibid.* **28**, 1026 (1983); R. J. Lad and V. E. Henrich, *ibid.* **39**, 13478 (1989); M. R. Thuler, R. L. Benbow and Z. Hurych, *ibid.* **27**, 2082 (1983); J. Ghijsen, L. H. Tjeng, H. Eskes, G. A. Sawatzky, and R. L. Johnson, *ibid.* **42**, 2268 (1990).
- ¹⁴L. C. Davis, J. Appl. Phys. **59**, R25 (1986).
- ¹⁵G. A. Sawatzky, in *Core-Level Spectroscopy in Condensed Systems*, edited by J. Kanamori and A. Kotani (Springer-Verlag, Berlin, 1988), p. 99.
- ¹⁶A. Fujimori, in *Core-Level Spectroscopy in Condensed Systems*, edited by J. Kanamori and A. Katani (Springer-Verlag, Berlin, 1988), p. 136.
- ¹⁷R. Kelly, Mat. Sci. Eng. **A115**, 11 (1989).
- ¹⁸V. M. Bermudez and V. H. Ritz, Chem. Phys. Lett. **73**, 160 (1980).
- ¹⁹W. Göpel and G. Rucker, J. Vac. Sci. Technol. **21**, 389 (1982); W. Göpel, G. Rucker, and R. Feierabend, Phys. Rev. B **28**, 3427 (1983).
- ²⁰M. Iwamoto, Y. Yoda, M. Egashira, and T. Seiyama, J. Phys. Chem. **80**, 1989 (1976); M. Iwamoto, Y. Yoda, N. Yamazoe, and T. Seiyama, Bull. Chem. Soc. Jpn. **51**, 2765 (1978).
- ²¹M. Che and A. J. Tench, Adv. Catal. **31**, 77 (1982).
- ²²A. Bielauski and J. Haber, Adv. Catal. **19**, 1 (1979).